SIAM J. NUMER. ANAL.
Vol. 50, No. 1, pp. 105–125

SECOND-ORDER CONVEX SPLITTING SCHEMES FOR GRADIENT FLOWS WITH EHRLICH–SCHWOEBEL TYPE ENERGY: APPLICATION TO THIN FILM EPITAXY*

JIE SHEN†, CHENG WANG‡, XIAOMING WANG§, AND STEVEN M. WISE¶

Abstract. We construct unconditionally stable, unconditionally uniquely solvable, and second-order accurate (in time) schemes for gradient flows with energy of the form $\int_\Omega (F(\nabla\phi(\mathbf{x}))+\frac{\epsilon^2}{2}|\Delta\phi(\mathbf{x})|^2)\,d\mathbf{x}$. The construction of the schemes involves the appropriate combination and extension of two classical ideas: (i) appropriate convex-concave decomposition of the energy functional and (ii) the secant method. As an application, we derive schemes for epitaxial growth models with slope selection ($F(\mathbf{y}) = \frac{1}{4}(|\mathbf{y}|^2-1)^2$) or without slope selection ($F(\mathbf{y}) = -\frac{1}{2}\ln(1+|\mathbf{y}|^2)$). Two types of unconditionally stable uniquely solvable second-order schemes are presented. The first type inherits the variational structure of the original continuous-in-time gradient flow, while the second type does not preserve the variational structure. We present numerical simulations for the case with slope selection which verify well-known physical scaling laws for the long time coarsening process.

Key words. unconditional stability, second order scheme, convex-concave decomposition, epitaxial growth, Ehrlich–Schwoebel type energy

AMS subject classifications. 65M12, 37L65, 65M06, 65M70, 65Z05, 37L15

DOI. 10.1137/110822839

1. Introduction.

Coarsening, i.e., the process by which a group of objects of different sizes transforms into a group consisting of fewer objects with larger average size, is a very common natural phenomenon and has attracted considerable attention recently [9]. The coarsening process usually takes place on a very long time scale for large systems [10]. Therefore it is important to have accurate and efficient time stepping with regard to numerical simulation.

Many phenomenological macroscopic coarsening processes are energy driven in the sense that the dynamics is the gradient flow of a certain "energy functional" [15, 16]. One well-known example associated with epitaxial thin film growth is the gradient flow with the "energy" taking the (nondimensionalized) form

$$E(\phi) = \int_\Omega \left(F(\nabla\phi(\mathbf{x})) + \frac{\epsilon^2}{2}|\Delta\phi(\mathbf{x})|^2 \right) d\mathbf{x}, \tag{1.1}$$

*Received by the editors January 31, 2011; accepted for publication (in revised form) November 8, 2011; published electronically January 26, 2012. Part of this work was carried out while the first and third authors were visiting the Institute for Mathematics and its Applications at the University of Minnesota in the spring of 2010.

http://www.siam.org/journals/sinum/50-1/82283.html

†Department of Mathematics, Purdue University, West Lafayette, IN 47907-2067 (shen7@math.purdue.edu). The work of this author was supported in part of NSF grant DMS-0915066 and AFOSR FA9550-08-1-0416.

‡Department of Mathematics, University of Massachusetts, Dartmouth, North Dartmouth, MA 02747-2300 (cwang1@umassd.edu). The work of this author was supported in part by NSF grants DCNS-0959382 and DMS-1115420 and AFOSR 10418149.

§Corresponding author. Department of Mathematics, Florida State University, Tallahassee, FL 32306-4510 (wxm@math.fsu.edu). The work of this author was supported in part by NSF grants DMS-0606671 and DMS-1008852 and by a grant from the Chinese MOE through the 111 Project of Modern Applied Mathematics at Fudan University.

¶Department of Mathematics, University of Tennessee, Knoxville, TN 37996-1300 (swise@math.tuk.edu). The work of this author was supported in part by NSF grants DMS-0818030 and DMS-1115390.

where $F(\mathbf{y})$ is a smooth function of its argument $\mathbf{y}$, $\Omega = \mathbb{T}^d$ is the d dimensional periodic box with period 2π and $d \geq 2$, $\phi : \Omega \to \mathbb{R}$ is a periodic height function (in a moving reference frame) with average zero, and ϵ is a constant (inversely proportional to the size of the system). The first term,

$$E_{ES}(\phi) := \int_\Omega F(\nabla_{\mathbf{x}}\phi(\mathbf{x}))\, d\mathbf{x}, \tag{1.2}$$

represents a continuum description of the Ehrlich–Schwoebel effect—according to which adatoms (absorbed atoms) must overcome a higher energy barrier to stick to a step from an upper rather than from a lower terrace [8, 24]—while the second term,

$$E_{SD}(\phi) := \int_\Omega \frac{\epsilon^2}{2}|\Delta\phi(\mathbf{x})|^2\, d\mathbf{x}, \tag{1.3}$$

represents the surface diffusion effect. The case with higher order diffusion as well as Neumann-type boundary condition ($\frac{\partial\phi}{\partial n}\big|_{\partial\Omega} = \frac{\partial\Delta\phi}{\partial n}\big|_{\partial\Omega} = 0$) can be considered as well [10, 19].

There are two popular choices for the Ehrlich–Schwoebel energy (1.2): the *case without slope selection*,

$$E_1(\phi) = \int_\Omega \left(-\frac{1}{2}\ln(1+|\nabla\phi|^2) + \frac{\epsilon^2}{2}|\Delta\phi|^2\right) d\mathbf{x}, \tag{1.4}$$

and the *case with slope selection*,

$$E_2(\phi) = \int_\Omega \left(\frac{1}{4}\Big(|\nabla\phi|^2 - 1\Big)^2 + \frac{\epsilon^2}{2}|\Delta\phi|^2\right) d\mathbf{x}. \tag{1.5}$$

The second energy may be viewed as an approximation of the first energy under the assumption that the gradient of the height is small [20]. There are significant differences between the two models with the second (simplified) model having a slope selection mechanism (structures with $|\nabla\phi| = 1$ are preferred) that is absent in the first model. This leads to differences in energy minimizers and long time coarsening processes [15, 17, 20].

The variational derivatives of these functionals, which may be interpreted as chemical potentials, can be calculated formally as

$$\mu := \frac{\delta E}{\delta\phi} = -\nabla_{\mathbf{x}}\cdot\nabla_{\mathbf{y}}F(\nabla_{\mathbf{x}}\phi) + \epsilon^2\Delta^2\phi. \tag{1.6}$$

The gradient flow then takes the form

$$\frac{\partial\phi}{\partial t} = -M\mu = M\left(\nabla_{\mathbf{x}}\cdot\nabla_{\mathbf{y}}F(\nabla_{\mathbf{x}}\phi) - \epsilon^2\Delta^2\phi\right), \tag{1.7}$$

where $M > 0$ is a mobility, which can be always set to 1 ($M = 1$) by rescaling the time. Periodic boundary conditions are assumed for ϕ in both spatial directions for simplicity.

The physically interesting coarsening process for spatially large systems (small ϵ) occurs on a very long time scale. For instance, for the model with slope selection, the minimal energy is of the order of ϵ [15]. Assuming the widely believed $t^{-\frac{1}{3}}$ scaling for the energy [17, 20, 21], it requires about $\frac{1}{\epsilon^3}$ time for the system to reach saturation from an initially order one profile. (The saturation time would be of the order of ϵ^{-2} under the scaling that we have adopted for our equation.) Therefore, numerical

simulations for the coarsening process of large systems require long time accuracy and stability. In particular, higher order (with respect to time discretization) schemes are very desirable. In addition, unconditional energy stability is also coveted, since one would like to have the capability of preserving the stability even if large time steps are taken (in adaptive time stepping for instance).

Various first-order unconditionally energy stable schemes for models of thin film epitaxial growth were derived recently [4, 30]. The purpose of this manuscript is to construct convex splitting schemes that are second-order in time, uniquely solvable, and unconditionally energy stable for gradient flows with Ehrlich–Schwoebel type energy and to apply them to models of thin film epitaxy. We note that second-order, uniquely solvable, and unconditionally energy stable schemes have been constructed recently in [31] for Swift–Hohenberg and phase field crystal type equations. The schemes in [31] can be applied to Allen–Cahn and Cahn–Hilliard type equations, as well as other gradient flows where the nonlinearity involves only the height function. (We refer to [6, 25, 26, 33, 5, 29] for other related convexity splitting schemes.) It is not obvious whether any of the schemes from the works just mentioned can be extended to gradient flows with an Ehrlich–Schwoebel type energy that is a function of the gradient of the height function (instead of the height function only). We also point out that efficient first-, second-, and third-order in time accurate schemes have been investigated in [32], where the authors derived energy stability for their first-order scheme under certain assumption on the numerically computed solution itself.

The rest of the paper is organized as follows. In section 2 we present and analyze a family of second-order in time, uniquely solvable, unconditionally energy stable schemes that preserves the variational structure of the continuous in time model. We introduce alternative schemes with all the desired properties except the variational structure in section 3. Section 4 is devoted to specific applications to the models of thin film epitaxial growth with or without slope selection. Fully discretized schemes are discussed in section 5. We specifically discuss three space discretization methods, including finite difference, Galerkin–Fourier-spectral, and collocation Fourier-spectral methods. Numerical results—obtained using the finite difference method in space and the time stepping proposed in section 2—applied to the case with slope selection are presented in section 6. We offer our concluding remarks in section 7.

2. The scheme with variational structure. Without loss of generality, we assume that the Ehrlich–Schwoebel type energy density $F(\mathbf{y})$ is smooth and possesses a convex (+, concave −, respectively) splitting with a quadratic concave term, i.e.,

$$F(\mathbf{y}) = F_+(\mathbf{y}) + F_-(\mathbf{y}) \quad \text{with} \quad F_-(\mathbf{y}) = -C|\mathbf{y}|^2. \tag{2.1}$$

The philosophy we shall use to construct a second-order energy stable scheme is a combination of the convex-concave splitting (see [12], for instance) and the secant method (see, for instance, [6]) modified so that it can be applied to the vector form and utilized on the convex part only.

Following the general idea of treating the convex part implicitly and the concave part explicitly, a second-order convex splitting scheme should take the following form for the gradient flow (1.7):

$$\begin{aligned} &\frac{\phi^{n+1}-\phi^n}{k}+\frac{\epsilon^2}{2}\Delta^2(\phi^{n+1}+\phi^n)+\nabla_{\mathbf{x}}\cdot H_n^{n+1}(F_+) \\ &\qquad = \nabla_{\mathbf{x}}\cdot\left(\frac{3}{2}\nabla_{\mathbf{y}}F_-(\nabla_{\mathbf{x}}\phi^n)-\frac{1}{2}\nabla_{\mathbf{y}}F_-(\nabla_{\mathbf{x}}\phi^{n-1})\right), \end{aligned} \tag{2.2}$$

where $H_n^{n+1}(F_+)$ should be chosen such that the above scheme is second-order at $t_{n+\frac{1}{2}}$ and energy stable. Since the energy stability is usually proved by taking the inner product of the above with $(\phi^{n+1}-\phi^n)$, the following inequality has to be satisfied:

$$(H_n^{n+1}(F_+), \nabla(\phi^{n+1}-\phi^n)) \geq \int_\Omega F_+(\nabla\phi^{n+1})\,d\mathbf{x} - \int_\Omega F_+(\nabla\phi^n)\,d\mathbf{x}. \tag{2.3}$$

Let us set $\mathbf{y}^m = \nabla_{\mathbf{x}}\phi^m$. Then, by direct calculation, we have

$$\begin{aligned}
&\int_\Omega F_+(\nabla\phi^{n+1})\,d\mathbf{x} - \int_\Omega F_+(\nabla\phi^n)\,d\mathbf{x}\\
&\quad= \int_\Omega\int_0^1 \frac{d}{d\tau}F_+(\mathbf{y}^n+\tau(\mathbf{y}^{n+1}-\mathbf{y}^n))\,d\tau\,d\mathbf{x}\\
&\quad= \int_\Omega\int_0^1 \nabla_{\mathbf{y}}F_+(\mathbf{y}^n+\tau(\mathbf{y}^{n+1}-\mathbf{y}^n))\,d\tau\cdot(\mathbf{y}^{n+1}-\mathbf{y}^n)\,d\mathbf{x}\\
&\quad= -\int_\Omega \nabla_{\mathbf{x}}\cdot\left(\int_0^1 \nabla_{\mathbf{y}}F_+(\mathbf{y}^n+\tau(\mathbf{y}^{n+1}-\mathbf{y}^n))\,d\tau\right)(\phi^{n+1}-\phi^n)\,d\mathbf{x}.
\end{aligned} \tag{2.4}$$

Therefore, a natural choice for H_n^{n+1} is

$$H_n^{n+1}(F_+) = -\nabla_{\mathbf{x}}\cdot\left(\int_0^1 \nabla_{\mathbf{y}}F_+(\mathbf{y}^n+\tau(\mathbf{y}^{n+1}-\mathbf{y}^n))\,d\tau\right), \tag{2.5}$$

and our second-order convex splitting scheme is

$$\begin{aligned}
&\frac{\phi^{n+1}-\phi^n}{k} + \frac{\epsilon^2}{2}\Delta^2(\phi^{n+1}+\phi^n) - \nabla_{\mathbf{x}}\cdot\left(\int_0^1 \nabla_{\mathbf{y}}F_+(\mathbf{y}^n+\tau(\mathbf{y}^{n+1}-\mathbf{y}^n))\,d\tau\right)\\
&\qquad= \nabla_{\mathbf{x}}\cdot\left(\frac{3}{2}\nabla_{\mathbf{y}}F_-(\nabla_{\mathbf{x}}\phi^n) - \frac{1}{2}\nabla_{\mathbf{y}}F_-(\nabla_{\mathbf{x}}\phi^{n-1})\right).
\end{aligned} \tag{2.6}$$

Alternatively, we can write the above scheme in the weak form: find $\phi^{n+1}\in \dot{H}^2_{per}(\Omega) := \{\phi\in H^2(\Omega) : \phi \text{ is periodic with average zero}\}$ such that

$$\begin{aligned}
&\left(\frac{\phi^{n+1}-\phi^n}{k},\psi\right) + \left(\frac{\epsilon^2}{2}\Delta(\phi^{n+1}+\phi^n),\Delta\psi\right)\\
&\qquad + \left(\int_0^1 \nabla_{\mathbf{y}}F_+(\mathbf{y}^n+\tau(\mathbf{y}^{n+1}-\mathbf{y}^n))\,d\tau, \nabla_{\mathbf{x}}\psi\right)\\
&\qquad = \left(\frac{3}{2}\nabla_{\mathbf{y}}F_-(\nabla_{\mathbf{x}}\phi^n) - \frac{1}{2}\nabla_{\mathbf{y}}F_-(\nabla_{\mathbf{x}}\phi^{n-1}), \nabla_{\mathbf{x}}\psi\right) \quad \forall\psi\in\dot{H}^2_{per}(\Omega),
\end{aligned} \tag{2.7}$$

where $\mathbf{y}^{n+1} = \nabla_{\mathbf{x}}\phi^{n+1}$ and $\mathbf{y}^n = \nabla_{\mathbf{x}}\phi^n$.

Note that the treatment of the concave part is unique in the following sense: for quadratic energy, this is the only way to get second-order accuracy with an explicit two-step treatment. The treatment of the diffusion term is not unique. We have utilized the midpoint rule corresponding to the Crank–Nicolson approach. Alternative approximations, such as $\frac{3}{4}\Delta^2\phi^{n+1} + \frac{1}{4}\Delta^2\phi^{n-1}$, can be used as well if more dissipation is desired.

The main result of this section is the following theorem.

THEOREM 2.1. *Under the assumption* (2.1)*, the scheme* (2.7) *is second-order accurate in time and unconditionally stable. More precisely, we have*

(2.8)
$$E(\phi^{n+1}) + \frac{C}{2}\|\nabla(\phi^{n+1}-\phi^n)\|^2 + \frac{\|\phi^{n+1}-\phi^n\|^2}{k} + \frac{C}{2}\|\nabla(\phi^{n+1}+\phi^{n-1}-2\phi^n)\|^2 = E(\phi^n) + \frac{C}{2}\|\nabla(\phi^n-\phi^{n-1})\|^2.$$

Moreover, at each time step, the scheme corresponds to the Euler–Lagrange equation for the following strictly convex coercive variation problem:

$$E_{scheme}(\phi,\phi^n,\phi^{n-1}) = \frac{\epsilon^2}{2}\|\Delta\phi\|^2 + \frac{1}{2k}\|\phi\|^2 + \int_\Omega \mathcal{F}_p(\nabla\phi,\nabla\phi^n)\,d\mathbf{x} + \int_\Omega \left(-\nabla\cdot\left(\frac{3}{2}\nabla_{\mathbf{y}}F_-(\nabla\phi^n) - \frac{1}{2}\nabla_{\mathbf{y}}F_-(\nabla\phi^{n-1})\right) + \frac{\epsilon^2}{2}\Delta^2\phi^n - \frac{\phi^n}{k}\right)\phi\,d\mathbf{x} \tag{2.9}$$

with

$$\mathcal{F}_p(\nabla\phi,\nabla\phi^n) = \int_0^1 \frac{1}{\tau}\left(F_+(\nabla\phi^n + \tau(\nabla\phi-\nabla\phi^n)) - F_+(\nabla\phi^n)\right)\,d\tau. \tag{2.10}$$

Therefore, the scheme is uniquely solvable provided that $F_+(\mathbf{y})$ *and* $\nabla_{\mathbf{y}}F_+(\mathbf{y})$ *grow most like a polynomial in* $\mathbf{y}$.

Proof. By taking the Taylor expansion at $t_{n+\frac{1}{2}}$, it is straightforward to see that the scheme is second-order accurate in time. We omit the details for the sake of brevity.

The unconditional stability of the scheme is guaranteed by the discrete energy law (2.8). In order to derive this discrete energy law, we take $\psi = \phi^{n+1}-\phi^n$ in (2.7).

Obviously, we have

$$\int_\Omega -\frac{\epsilon^2}{2}\Delta^2(\phi^{n+1}+\phi^n)(\phi^{n+1}-\phi^n)\,d\mathbf{x} = -\frac{\epsilon^2}{2}\int_\Omega (|\Delta\phi^{n+1}|^2 - |\Delta\phi^n|^2)\,d\mathbf{x}. \tag{2.11}$$

Thanks to the assumption (2.1), we have $\nabla_{\mathbf{y}}F_-(\mathbf{y}) = -2C\mathbf{y}$. Therefore,

$$\begin{aligned}
&-\int_\Omega \left(\frac{3}{2}\nabla_{\mathbf{y}}F_-(\nabla_{\mathbf{x}}\phi^n) - \frac{1}{2}\nabla_{\mathbf{y}}F_-(\nabla_{\mathbf{x}}\phi^{n-1})\right)\cdot\nabla_{\mathbf{x}}(\phi^{n+1}-\phi^n)\,d\mathbf{x}\\
&= C\int_\Omega (3\nabla\phi^n - \nabla\phi^{n-1})\cdot(\nabla\phi^{n+1}-\nabla\phi^n)\,d\mathbf{x}\\
&= 2C\int_\Omega \nabla\phi^n\cdot(\nabla\phi^{n+1}-\nabla\phi^n)\,d\mathbf{x} + C\int_\Omega (\nabla\phi^n-\nabla\phi^{n-1})\cdot(\nabla\phi^{n+1}-\nabla\phi^n)\,d\mathbf{x}\\
&= C\int_\Omega \big(-|\nabla\phi^n|^2 + |\nabla\phi^{n+1}|^2 - |\nabla(\phi^{n+1}-\phi^n)|^2 + (\nabla\phi^n-\nabla\phi^{n-1})\\
&\qquad\cdot(\nabla\phi^{n+1}-\nabla\phi^n)\big)\,d\mathbf{x}\\
&= C\int_\Omega \left(-|\nabla\phi^n|^2 + |\nabla\phi^{n+1}|^2 - \frac{1}{2}|\nabla(\phi^{n+1}-\phi^n)|^2 + \frac{1}{2}|\nabla\phi^n-\nabla\phi^{n-1}|^2\right)\\
&- C\int_\Omega \frac{1}{2}|\nabla(\phi^{n+1}+\phi^{n-1}-2\phi^n)|^2\,d\mathbf{x}.
\end{aligned} \tag{2.12}$$

Combining the above two inequalities and (2.4), we deduce the desired discrete energy law (2.8).

On the other hand, we can easily verify that

$$\nabla_{\mathbf{x}} \cdot \left(\int_0^1 \nabla_{\mathbf{y}} F_+(\mathbf{y}^n + \tau(\mathbf{y}^{n+1} - \mathbf{y}^n))\, d\tau \right) = -\frac{\delta \int_\Omega \mathcal{F}_p(\nabla\phi^{n+1}, \nabla\phi^n)\, d\mathbf{x}}{\delta\phi^{n+1}}. \tag{2.13}$$

Therefore the scheme (2.6) is the Euler–Lagrange equation of the energy functional given in (2.9). The convexity of $\mathcal{F}_p$ follows from the convexity of

$$\frac{1}{\tau}\left(F_+(\nabla\phi^n + \tau(\nabla\phi - \nabla\phi^n)) - F_+(\nabla\phi^n)\right)$$

for all $\tau \in (0, 1]$, thanks to the convexity of F_+. In turn, the coercivity of the energy functional (2.9) then follows from the convexity of $\mathcal{F}_p$ and the diffusion term. Therefore, the unique solution to the scheme exists and is the unique minimizer of the energy functional (2.9) under usual differentiability and growth conditions on F_+ [7, 11, 13]. ∎

3. Alternative schemes without variational structure. Alternative second-order unconditionally stable and uniquely solvable schemes do exist if we do not care about the preservation of the variational structure. In this case, straightforward generalization of the secant method would work without involving the integral form that we used in deriving the scheme with variational structure that we presented in the previous section. The resulting schemes are generally more compact than the schemes derived in the previous section, although they lack the variational structure. Here we illustrate two alternative ways of deriving second-order unconditionally stable and uniquely solvable schemes for equations of thin film epitaxial growth with or without slope selection.

Without loss of generality, we assume that the Ehrlich–Schwoebel type energy density $F(\mathbf{y})$ is smooth and takes the form

$$F(\mathbf{y}) = G(|\mathbf{y}|^2). \tag{3.1}$$

This certainly fits the thin film epitaxy models that we are interested in here with $G(\xi) = -\frac{1}{2}\ln(1+\xi)$ for the case without slope selection and $G(\xi) = \frac{1}{4}(\xi - 1)^2$ for the case with slope selection.

Following the general convex-splitting idea (see, for instance, [12, 30]), we assume that it possesses a convex-concave splitting with a quadratic concave term, i.e.,

$$G(\xi) = G_+(\xi) + G_-(\xi) \quad \text{with} \quad G_+'' \geq 0, \quad G_+' \geq 0, \quad \text{and} \quad G_-(\xi) = -C\xi. \tag{3.2}$$

We now construct a scheme with the following considerations: (i) the concave quadratic term associated with G_- can be treated explicitly via a classical two-level method as before in order to preserve the energy law and maintain the second-order accuracy; (ii) likewise, the convex quadratic term $(\frac{\epsilon^2}{2}\|\Delta\phi|^2)$ can be treated easily using classical midpoint type approximation; (iii) for the convex part associated with G_+, we mimic the classical secant method for second-order approximation (see, for instance, [6]) in this vector setting. Taking into account the above considerations, we arrive at the following second-order scheme:

$$\begin{aligned} \frac{\phi^{n+1} - \phi^n}{k} &= \nabla \cdot \left(\frac{G_+(|\nabla\phi^{n+1}|^2) - G_+(|\nabla\phi^n|^2)}{|\nabla\phi^{n+1}|^2 - |\nabla\phi^n|^2} (\nabla\phi^{n+1} + \nabla\phi^n) \right) \\ &\quad + \nabla \cdot \left(3G_-'(|\nabla\phi^n|^2)\nabla\phi^n - G_-'(|\nabla_{\mathbf{x}}\phi^{n-1}|^2)\nabla\phi^{n-1} \right) - \frac{\epsilon^2}{2}\Delta^2(\phi^{n+1} + \phi^n). \end{aligned} \tag{3.3}$$

The weak form of the above scheme is as follows: find $\phi^{n+1} \in \dot{H}^2_{per}(\Omega)$ such that

$$\begin{aligned}(3.4)\quad &\left(\frac{\phi^{n+1}-\phi^n}{k},\psi\right)+\left(\frac{\epsilon^2}{2}\Delta(\phi^{n+1}+\phi^n),\Delta\psi\right)\\ &\quad+\left(\frac{G_+(|\nabla\phi^{n+1}|^2)-G_+(|\nabla\phi^n|^2)}{|\nabla\phi^{n+1}|^2-|\nabla\phi^n|^2}(\nabla\phi^{n+1}+\nabla\phi^n),\nabla\psi\right)\\ &\quad=\left(3G'_-(|\nabla\phi^n|^2)\nabla\phi^n-G'_-(|\nabla_{\mathbf{x}}\phi^{n-1}|^2)\nabla\phi^{n-1},\nabla\psi\right)\quad\forall\psi\in\dot{H}^2_{per}(\Omega).\end{aligned}$$

THEOREM 3.1. *Under the assumption* (3.2)*, the alternative scheme* (3.3) *is second-order accurate in time, unconditionally energy stable in the sense that*

$$\begin{aligned}(3.5)\quad &E(\phi^{n+1})+\frac{C}{2}\|\nabla(\phi^{n+1}-\phi^n)\|^2+\frac{\|\phi^{n+1}-\phi^n\|^2}{k}\\ &\quad+\frac{C}{2}\|\nabla(\phi^{n+1}+\phi^{n-1}-2\phi^n)\|^2=E(\phi^n)+\frac{C}{2}\|\nabla(\phi^n-\phi^{n-1})\|^2.\end{aligned}$$

Moreover, for the case of an energy functional given by the model with slope selection (1.5)*, and with the splitting given by* $G_+(\xi)=\frac{1}{4}\xi^2+\frac{1}{4}, G_-(\xi)=-\frac{1}{2}\xi$*, the scheme is uniquely solvable.*

Proof. Again, the second-order accuracy of this scheme (3.4) can be verified by taking the Taylor expansion at $t_{n+\frac{1}{2}}$.

In order to prove the energy law (3.5), we take $\psi=\phi^{n+1}-\phi^n$ in (3.4). Notice that with the assumption (3.2), the contribution of the concave part is exactly the same as in (2.12). Thus, the energy law (3.5) follows similarly.

To prove the unique solvability, we need the following lemma.

LEMMA 3.2. *Consider the (nonlinear) problem*

$$(3.6)\qquad \frac{\phi}{k}-\nabla\cdot\mathcal{F}(\nabla\phi,\mathbf{x})+\frac{\epsilon^2}{2}\Delta^2\phi=f,$$

where $\mathcal{F}, f$ *are given (smooth) functions. Then a sufficient condition on uniqueness (of sufficiently smooth solutions) is that the symmetric part of the Jacobian of* $\mathcal{F}$ *is nonnegative.*

Proof of Lemma 3.2. Suppose we have two solutions $\phi,\tilde{\phi}$ to the general scheme (3.6). Then, we have

$$\frac{\phi-\tilde{\phi}}{k}-\nabla\cdot(\mathcal{F}(\nabla\phi,\mathbf{x})-\mathcal{F}(\nabla\tilde{\phi},\mathbf{x}))+\frac{\epsilon^2}{2}\Delta^2(\phi-\tilde{\phi})=0.$$

Taking the inner product of this equation with $\phi-\tilde{\phi}$, we deduce

$$\begin{aligned}0&=\frac{\|\phi-\tilde{\phi}\|^2}{k}+\int_\Omega(\mathcal{F}(\nabla\phi,\mathbf{x})-\mathcal{F}(\nabla\tilde{\phi},\mathbf{x}))\cdot\nabla(\phi-\tilde{\phi})\,d\mathbf{x}+\frac{\epsilon^2}{2}\|\Delta(\phi-\tilde{\phi})\|^2\\ &=\frac{\|\phi-\tilde{\phi}\|^2}{k}+\int_\Omega\int_0^1(J(\mathcal{F})(\nabla\tilde{\phi}+\tau\nabla(\phi-\tilde{\phi}),\mathbf{x})\nabla(\phi-\tilde{\phi}))\,d\tau\\ &\quad\cdot\nabla(\phi-\tilde{\phi})\,d\mathbf{x}+\frac{\epsilon^2}{2}\|\Delta(\phi-\tilde{\phi})\|^2\\ &\geq\frac{\|\phi-\tilde{\phi}\|^2}{k}+\frac{\epsilon^2}{2}\|\Delta(\phi-\tilde{\phi})\|^2,\end{aligned}$$

where in the last step we have used the assumption that the symmetric part of the Jacobian of $\mathcal{F}$ is nonnegative. ∎

It is now straightforward to prove the unique solvability stated in the theorem. Indeed, with the specific choice of G_+ and G_-, we have

$$\begin{aligned} &J(\mathcal{F}(\mathbf{y})) \\ &= \int_0^1 \int_0^s G_+''(|\mathbf{y}|^2 + \tau(|\mathbf{y}_0|^2 - |\mathbf{y}|^2))[|\mathbf{y}_0|^2 - |\mathbf{y}|^2 + 2\mathbf{y} \otimes (\mathbf{y} + \mathbf{y}_0)]\, d\tau ds + G'(|\mathbf{y}|^2) I \\ &= \frac{1}{4}\left((|\mathbf{y}_0|^2 + |\mathbf{y}|^2) I + (\mathbf{y} + \mathbf{y}_0) \otimes (\mathbf{y} + \mathbf{y}_0) + \mathbf{y} \otimes \mathbf{y} - \mathbf{y}_0 \otimes \mathbf{y}_0 + (\mathbf{y} \otimes \mathbf{y}_0 - \mathbf{y}_0 \otimes \mathbf{y})\right). \end{aligned}$$

It is then straightforward to see that the symmetric part of this Jacobian matrix is nonnegative.

Notice that this Jacobian matrix is nonsymmetric in general. Therefore, we can conclude that the term $\nabla_{\mathbf{x}} \mathcal{F}(\nabla \phi^{n+1})$ cannot be interpreted as the variational derivative of any energy functional of $\nabla \phi^{n+1}$ since that would imply the symmetry of the Jacobian. ∎

The scheme (3.3), while being more compact than the scheme (2.6), is only guaranteed to be uniquely solvable for the energy with slope selection (1.5). At the expense of compactness we can construct a second-order unconditionally stable, uniquely solvable scheme for more general energy functional. In this case, we adapt the classical secant method for the convex term to our vector setting via splitting the direction and a symmetrization at the end. In the two-dimensional case, the scheme takes the following form:

$$\begin{aligned} \frac{\phi^{n+1} - \phi^n}{k} &= \partial_{x_1} \frac{F_+(\nabla \phi^{n+1}) - F_+(\psi^*) + F_+(\psi_*) - F_+(\nabla \phi^n)}{\partial_{x_1}(\phi^{n+1} - \phi^n)} \\ &\quad + \partial_{x_2} \frac{F_+(\nabla \phi^{n+1}) - F_+(\psi_*) + F_+(\psi^*) - F_+(\nabla \phi^n)}{\partial_{x_2}(\phi^{n+1} - \phi^n)} \\ &\quad + \nabla_{\mathbf{x}} \cdot \left(\frac{3}{2} \nabla_{\mathbf{y}} F_-(\nabla_{\mathbf{x}} \phi^n) - \frac{1}{2} \nabla_{\mathbf{y}} F_-(\nabla_{\mathbf{x}} \phi^{n-1})\right) - \frac{\epsilon^2}{2} \Delta^2(\phi^{n+1} + \phi^n), \end{aligned} \tag{3.7}$$

where

$$\psi^* = (\partial_{x_1} \phi^n, \partial_{x_2} \phi^{n+1}), \psi_*(\partial_{x_1} \phi^{n+1}, \partial_{x_2} \phi^n).$$

The scheme for the three-dimensional case can be constructed accordingly.

It is straightforward to verify that this scheme is second-order accurate, unconditionally stable, and uniquely solvable with the convex-concave decomposition as before. It can also be verified that the scheme (3.7) coincides with the scheme (3.3) for the model with slope selection using the convex-concave splitting given in (4.1). Therefore, this scheme does not possesses variational structure. We leave the details to the interested reader.

4. Application to thin film epitaxy.

4.1. Case with slope selection. In this case, a convenient splitting of the Ehrlich–Schwoebel energy density $F(\mathbf{y}) = \frac{1}{4}(|\mathbf{y}|^2 - 1)^2$ is

$$F_+(\mathbf{y}) = \frac{1}{4}|\mathbf{y}|^4 + \frac{1}{4}, \quad F_-(\mathbf{y}) = -\frac{1}{2}|\mathbf{y}|^2. \tag{4.1}$$

We can explicitly calculate the (variational) potential defined in (2.10) associated with the convex part of the scheme as

$$\begin{aligned}
&\mathcal{F}_p(\mathbf{y},\mathbf{y}_0)\\
&\quad=\int_0^1 \frac{1}{4\tau}(|\mathbf{y}_0+\tau(\mathbf{y}-\mathbf{y}_0)|^4-|\mathbf{y}_0|^4)\,d\tau\\
&\quad=\int_0^1 \frac{1}{4}(|\mathbf{y}_0+\tau(\mathbf{y}-\mathbf{y}_0)|^2+|\mathbf{y}_0|^2)(2\mathbf{y}_0+\tau(\mathbf{y}-\mathbf{y}_0))\cdot(\mathbf{y}-\mathbf{y}_0)\,d\tau\\
&\quad=\int_0^1 \frac{1}{4}(2|\mathbf{y}_0|^2+2\tau\mathbf{y}_0\cdot(\mathbf{y}-\mathbf{y}_0)+\tau^2|\mathbf{y}-\mathbf{y}_0|^2)(2\mathbf{y}_0\cdot(\mathbf{y}-\mathbf{y}_0)+\tau|\mathbf{y}-\mathbf{y}_0|^2)\,d\tau\\
&\quad=\frac{1}{4}\bigg(4\mathbf{y}_0\cdot(\mathbf{y}-\mathbf{y}_0)|\mathbf{y}_0|^2+2(\mathbf{y}_0\cdot(\mathbf{y}-\mathbf{y}_0))^2\\
&\qquad\quad+\frac{4}{3}\mathbf{y}_0\cdot(\mathbf{y}-\mathbf{y}_0)|\mathbf{y}-\mathbf{y}_0|^2+|\mathbf{y}_0|^2|\mathbf{y}-\mathbf{y}_0|^2+\frac{1}{4}|\mathbf{y}-\mathbf{y}_0|^4\bigg)\\
&\quad=\frac{1}{4}\left(\frac{1}{4}|\mathbf{y}|^4+\frac{1}{3}\mathbf{y}_0\cdot\mathbf{y}|\mathbf{y}|^2+\frac{1}{6}|\mathbf{y}_0|^2|\mathbf{y}|^2+\frac{1}{3}(\mathbf{y}_0\cdot\mathbf{y})^2+\mathbf{y}_0\cdot\mathbf{y}|\mathbf{y}_0|^2-\frac{25}{12}|\mathbf{y}_0|^4\right). \qquad (4.2)
\end{aligned}$$

Therefore

$$\frac{\delta\mathcal{F}_p}{\delta\mathbf{y}}=\frac{1}{4}(|\mathbf{y}|^2\mathbf{y}+|\mathbf{y}_0|^2\mathbf{y}_0)+\frac{1}{12}(|\mathbf{y}|^2\mathbf{y}_0+|\mathbf{y}_0|^2\mathbf{y}+2(\mathbf{y}_0\cdot\mathbf{y})(\mathbf{y}+\mathbf{y}_0)). \qquad (4.3)$$

Thanks to (2.13), the scheme (2.6) becomes

$$\begin{aligned}
\frac{\phi^{n+1}-\phi^n}{k}&=\frac{1}{4}\nabla\cdot(|\nabla\phi^{n+1}|^2\nabla\phi^{n+1}+|\nabla\phi^n|^2\nabla\phi^n)\\
&\quad+\frac{1}{12}\nabla\cdot(|\nabla\phi^{n+1}|^2\nabla\phi^n+|\nabla\phi^n|^2\nabla\phi^{n+1}\\
&\qquad+2(\nabla\phi^n\cdot\nabla\phi^{n+1})(\nabla\phi^n+\nabla\phi^{n+1}))\\
&\quad-\Delta\left(\frac{3}{2}\phi^n-\frac{1}{2}\phi^{n-1}\right)-\frac{\epsilon^2}{2}\Delta^2(\phi^{n+1}+\phi^n). \qquad (4.4)
\end{aligned}$$

On the other hand, it is easy to check that in this case, the scheme (3.3) (alternatively, scheme (3.7)) takes the form

$$\begin{aligned}
\frac{\phi^{n+1}-\phi^n}{k}&=\frac{1}{4}\nabla\cdot[(|\nabla\phi^{n+1}|^2+|\nabla\phi^n|^2)(\nabla\phi^{n+1}+\nabla\phi^n)]\\
&\quad-\Delta\left(\frac{3}{2}\phi^n-\frac{1}{2}\phi^{n-1}\right)-\frac{\epsilon^2}{2}\Delta^2(\phi^{n+1}+\phi^n). \qquad (4.5)
\end{aligned}$$

Note that the above scheme is more compact than the scheme (4.4). In fact, the scheme (4.4) may be viewed as the symmetrization of the scheme (4.5).

4.2. Case without slope selection. In this case, a convenient convex-concave splitting of the Ehrlich–Schwoebel energy density $F(\mathbf{y})=-\frac{1}{2}\ln(1+|\mathbf{y}|^2)$ is [30]

$$F_+(\mathbf{y})=|\mathbf{y}|^2-\frac{1}{2}\ln(1+|\mathbf{y}|^2),\quad F_-(\mathbf{y})=-|\mathbf{y}|^2. \qquad (4.6)$$

It seems nontrivial to represent the (variational) potential $\mathcal{F}_p$ associated with the convex part using elementary functions. However, we note that only the variational

derivative is needed in the weak form of the scheme (2.7), and it can be calculated explicitly as follows:

$$
\begin{aligned}
&\int_0^1 (\nabla_{\mathbf{y}} F_+)(\mathbf{y}_0+\tau(\mathbf{y}-\mathbf{y}_0))\,d\tau \\
&\quad = \int_0^1 \left(2(\mathbf{y}_0+\tau(\mathbf{y}-\mathbf{y}_0)) - \frac{\mathbf{y}_0+\tau(\mathbf{y}-\mathbf{y}_0)}{1+|\mathbf{y}_0+\tau(\mathbf{y}-\mathbf{y}_0)|^2}\right) d\tau \\
&\quad = 2\mathbf{y}_0 + (\mathbf{y}-\mathbf{y}_0) - \int_0^1 \frac{\mathbf{y}_0+\tau(\mathbf{y}-\mathbf{y}_0)}{1+|\mathbf{y}_0+\tau(\mathbf{y}-\mathbf{y}_0)|^2}\,d\tau \\
&\quad = 2\mathbf{y}_0 + (\mathbf{y}-\mathbf{y}_0) \\
&\qquad - \frac{\mathbf{y}-\mathbf{y}_0}{2|\mathbf{y}-\mathbf{y}_0|} \ln \frac{\left(1+|\mathbf{y}_0|^2 - \frac{(\mathbf{y}_0\cdot(\mathbf{y}-\mathbf{y}_0))^2}{|\mathbf{y}-\mathbf{y}_0|^2}\right)^2 + \left(|\mathbf{y}-\mathbf{y}_0| + \frac{\mathbf{y}_0\cdot(\mathbf{y}-\mathbf{y}_0)}{|\mathbf{y}-\mathbf{y}_0|}\right)^2}{\left(1+|\mathbf{y}_0|^2 - \frac{(\mathbf{y}_0\cdot(\mathbf{y}-\mathbf{y}_0)}{|\mathbf{y}-\mathbf{y}_0|}\right)^2 + \left(\frac{\mathbf{y}_0\cdot(\mathbf{y}-\mathbf{y}_0)}{|\mathbf{y}-\mathbf{y}_0|}\right)^2} \\
&\qquad - \frac{\mathbf{y}_0|\mathbf{y}-\mathbf{y}_0| - (\mathbf{y}-\mathbf{y}_0)\frac{\mathbf{y}_0\cdot(\mathbf{y}-\mathbf{y}_0)}{|\mathbf{y}-\mathbf{y}_0|}}{(1+|\mathbf{y}_0|^2)|\mathbf{y}-\mathbf{y}_0|^2 - (\mathbf{y}_0\cdot(\mathbf{y}-\mathbf{y}_0))^2} \left(\tan^{-1} \frac{\frac{\mathbf{y}_0\cdot(\mathbf{y}-\mathbf{y}_0)}{|\mathbf{y}-\mathbf{y}_0|} + |\mathbf{y}-\mathbf{y}_0|}{1+|\mathbf{y}_0|^2 - \frac{(\mathbf{y}_0\cdot(\mathbf{y}-\mathbf{y}_0))^2}{|\mathbf{y}-\mathbf{y}_0|^2}} \right. \\
&\qquad\qquad \left. - \tan^{-1} \frac{\frac{\mathbf{y}_0\cdot(\mathbf{y}-\mathbf{y}_0)}{|\mathbf{y}-\mathbf{y}_0|}}{1+|\mathbf{y}_0|^2 - \frac{(\mathbf{y}_0\cdot(\mathbf{y}-\mathbf{y}_0))^2}{|\mathbf{y}-\mathbf{y}_0|^2}} \right),
\end{aligned}
\tag{4.7}
$$

where in the last step we have utilized the elementary calculus identity

$$
\int \frac{c_1+c_2\tau}{c_3^2+(c_4+c_5\tau)^2}\,d\tau = \frac{c_2}{2c_5}\ln(c_3^2+(c_4+c_5\tau)^2) + \frac{c_1c_5-c_2c_4}{c_3c_5^2}\arctan\frac{c_4+c_5\tau}{c_3}
$$

with $c_1=\mathbf{y}_0, c_2=\mathbf{y}-\mathbf{y}_0, c_5=|\mathbf{y}-\mathbf{y}_0|, c_4=\frac{\mathbf{y}_0\cdot(\mathbf{y}-\mathbf{y}_0)}{|\mathbf{y}-\mathbf{y}_0|}, c_3=1+|\mathbf{y}_0|^2-\frac{(\mathbf{y}_0\cdot(\mathbf{y}-\mathbf{y}_0))^2}{|\mathbf{y}-\mathbf{y}_0|^2}$.

This scheme enjoys the nice property of solvability and variational structure in any dimension on top of the second-order accuracy and unconditional energy stability at the expense of compactness. On the other hand, it is straightforward to write the explicit form for the scheme (3.7) which works in two dimensions, although without the variational structure.

5. Fully discrete schemes.

5.1. Spatial discretization via the finite difference method. This section defines finite difference versions of the schemes (4.4) and (4.5) for the slope selection equation

$$
\partial_t\phi = \nabla\cdot\left(|\nabla\phi|^2\nabla\phi\right) - \Delta\phi - \epsilon^2\Delta^2\phi. \tag{5.1}
$$

In contrast with Galerkin type methods—which we discuss in sections 5.2 and 5.3—finite difference methods require the careful definition of difference operators and grid functions in order to construct discrete-level versions of the PDE and the corresponding energy. This process is made difficult in the present case by the complicated form of the nonlinear 4-Laplacian operator $-\nabla\cdot(|\nabla\phi|^2\nabla\phi)$. Specifically, one must take extra care to derive a difference approximation that has a reasonably nice discrete energy. As is often the case with the finite difference method, the implementation of the scheme is rather simple. It is the analysis, via the appropriate discrete energy estimates, that is generally nontrivial.

We will follow the format of [31] somewhat. Let $\Omega = (0, L_x) \times (0, L_y)$, where $L_x = m_x \cdot h$ and $L_y = m_y \cdot h$, where $h > 0$. Set $p_i = (i - 1/2) \cdot h$ for i taking integer and half-integer values. Let $E_{m_x} = \{p_i \,|\, i = 1/2, 3/2, \ldots, m_x + 1/2\}$ and similarly for E_{m_y}. Define $C_{m_x} = \{p_i \,|\, i = 1, 2, \ldots, m_x\}$, $C^+_{m_x} = C_{m_x} \cup \{p_0, p_{m_x+1}\}$, and similarly for C_{m_y} and $C^+_{m_y}$. We define the following two-dimensional grid-function spaces:

$$\mathcal{V}_{m_x \times m_y} = \left\{u : E_{m_x} \times E_{m_y} \to \mathbb{R}\right\}, \tag{5.2}$$

$$\mathcal{C}_{m_x \times m_y} = \left\{\phi : C_{m_x} \times C_{m_y} \to \mathbb{R}\right\}, \quad \mathcal{C}^+_{m_x \times m_y} = \left\{\phi : C^+_{m_x} \times C^+_{m_y} \to \mathbb{R}\right\}, \tag{5.3}$$

$$\mathcal{E}^{\mathrm{ew}}_{m_x \times m_y} = \left\{f : E_{m_x} \times C_{m_y} \to \mathbb{R}\right\}, \quad \mathcal{E}^{\mathrm{ns}}_{m_x \times m_y} = \left\{f : C_{m_x} \times E_{m_y} \to \mathbb{R}\right\}. \tag{5.4}$$

The functions of $\mathcal{V}_{m_x \times m_y}$ (vertex grid functions) are identified via $u_{i+1/2,j+1/2} := u(p_{i+1/2}, p_{j+1/2})$, those of $\mathcal{C}_{m_x \times m_y}$ and $\mathcal{C}^+_{m_x \times m_y}$ (cell-centered grid functions) are identified via $\phi_{i,j} := \phi(p_i, p_j)$, those of $\mathcal{E}^{\mathrm{ew}}_{m_x \times m_y}$ (east-west edge-centered grid functions) are identified via $f_{i+1/2,j} := f(p_{i+1/2}, p_j)$, and, finally, those of $\mathcal{E}^{\mathrm{ns}}_{m_x \times m_y}$ (north-south edge-centered grid functions) are identified via $f_{i,j+1/2} := f(p_i, p_{j+1/2})$.

We define the operator $d_x : \mathcal{E}^{\mathrm{ew}}_{m_x \times m_y} \to \mathcal{C}_{m_x \times m_y}$ componentwise via

$$d_x f_{i,j} = \frac{1}{h}\left(f_{i+1/2,j} - f_{i-1/2,j}\right), \ {\scriptstyle i=1,\ldots,m_x \atop j=1,\ldots,m_y} \tag{5.5}$$

and define $D_x : \mathcal{C}^+_{m_x \times m_y} \to \mathcal{E}^{\mathrm{ew}}_{m_x \times m_y}$ componentwise via

$$D_x \phi_{i+1/2,j} = \frac{1}{h}\left(\phi_{i+1,j} - \phi_{i,j}\right), \ {\scriptstyle i=0,\ldots,m_x \atop j=1,\ldots,m_y}. \tag{5.6}$$

The operators $d_y : \mathcal{E}^{\mathrm{ns}}_{m_x \times m_y} \to \mathcal{C}_{m_x \times m_y}$ and $D_y : \mathcal{C}^+_{m_x \times m_y} \to \mathcal{E}^{\mathrm{ns}}_{m_x \times m_y}$ are defined analogously. The standard two-dimensional discrete Laplacian, $\Delta_h : \mathcal{C}^+_{m_x \times m_y} \to \mathcal{C}_{m_x \times m_y}$, is defined as

$$\begin{aligned} \Delta_h \phi_{i,j} &= d_x(D_x\phi)_{i,j} + d_y(D_y\phi)_{i,j} \\ &= \frac{1}{h^2}\left(\phi_{i+1,j} + \phi_{i-1,j} + \phi_{i,j+1} + \phi_{i,j-1} - 4\phi_{i,j}\right), \ {\scriptstyle i=1,\ldots,m_x \atop j=1,\ldots,m_y}. \end{aligned} \tag{5.7}$$

Define the center-to-vertex derivatives $\mathfrak{D}_x$, $\mathfrak{D}_y : \mathcal{C}^+_{m_x \times m_y} \to \mathcal{V}_{m_x \times m_y}$ componentwise as

$$\mathfrak{D}_x \phi_{i+1/2,j+1/2} := \frac{1}{2h}\left(\phi_{i+1,j+1} - \phi_{i,j+1} + \phi_{i+1,j} - \phi_{i,j}\right), \ {\scriptstyle i=0,\ldots,m_x \atop j=0,\ldots,m_y}, \tag{5.8}$$

$$\mathfrak{D}_y \phi_{i+1/2,j+1/2} := \frac{1}{2h}\left(\phi_{i+1,j+1} - \phi_{i+1,j} + \phi_{i,j+1} - \phi_{i,j}\right), \ {\scriptstyle i=0,\ldots,m_x \atop j=0,\ldots,m_y}. \tag{5.9}$$

The utility of these definitions is that the differences $\mathfrak{D}_x$ and $\mathfrak{D}_y$ are collocated on the grid, unlike the case for D_x, D_y. Define the vertex-to-center derivatives $\mathfrak{d}_x$, $\mathfrak{d}_y : \mathcal{V}_{m_x \times m_y} \to \mathcal{C}_{m_x \times m_y}$ componentwise as

$$\mathfrak{d}_x u_{i,j} := \frac{1}{2h}\left(u_{i+1/2,j+1/2} - u_{i-1/2,j+1/2} + u_{i+1/2,j-1/2} - u_{i-1/2,j-1/2}\right), \ {\scriptstyle i=1,\ldots,m_x \atop j=1,\ldots,m_y}, \tag{5.10}$$

$$\mathfrak{d}_y u_{i,j} := \frac{1}{2h}\left(u_{i+1/2,j+1/2} - u_{i+1/2,j-1/2} + u_{i-1/2,j+1/2} - u_{i-1/2,j-1/2}\right), \ {\scriptstyle i=1,\ldots,m_x \atop j=1,\ldots,m_y}. \tag{5.11}$$

We say the cell-centered function $\phi \in \mathcal{C}^+_{m_x \times m_y}$ is periodic if and only if

$$\phi_{m+1,j} = \phi_{1,j}, \quad \phi_{0,j} = \phi_{m,j}, \quad j = 1, \ldots, m_y, \tag{5.12}$$

$$\phi_{i,n+1} = \phi_{i,1}, \quad \phi_{i,0} = \phi_{i,n}, \quad i = 0, \ldots, m_x + 1. \tag{5.13}$$

A similar notion exists for periodic grid functions from $\mathcal{V}_{m_x \times m_y}$, $\mathcal{E}^{\mathrm{ew}}_{m_x \times m_y}$, and $\mathcal{E}^{\mathrm{ns}}_{m_x \times m_y}$ as well.

The first-order convex-splitting, finite difference scheme for the slope selection equation (5.1) scheme that was used (though not described) in [30] is the following: given $\phi^n \in \mathcal{C}^+_{m_x\times m_y}$ periodic, find $\phi^{n+1} \in \mathcal{C}^+_{m_x\times m_y}$ periodic such that

$$\phi^{n+1} - k\left[\mathfrak{d}_x\left\{r^{n+1}\mathfrak{D}_x\phi^{n+1}\right\} + \mathfrak{d}_y\left\{r^{n+1}\mathfrak{D}_y\phi^{n+1}\right\}\right] + k\epsilon^2\Delta_h w^{n+1} = \phi^n - k\Delta_h\phi^n, \tag{5.14}$$

where $r^{n+1} := (\mathfrak{D}_x\phi^{n+1})^2 + (\mathfrak{D}_y\phi^{n+1})^2 \in \mathcal{V}_{m_x\times m_y}$, and $w^{n+1} := \Delta_h\phi^{n+1} \in \mathcal{C}^+_{m_x\times m_y}$ is periodic. The finite difference version of the compact scheme (4.5) is precisely as follows: given ϕ^{n-1}, ϕ^n, $w^n \in \mathcal{C}^+_{m_x\times m_y}$ periodic, find $\phi^{n+1} \in \mathcal{C}^+_{m_x\times m_y}$ periodic such that

$$\begin{aligned}\phi^{n+1} - \frac{k}{4}\big[&\mathfrak{d}_x\left\{\left(r^{n+1}+r^n\right)\left(\mathfrak{D}_x\phi^{n+1}+\mathfrak{D}_x\phi^n\right)\right\}\\ &+\mathfrak{d}_y\left\{\left(r^{n+1}+r^n\right)\left(\mathfrak{D}_y\phi^{n+1}+\mathfrak{D}_y\phi^n\right)\right\}\big]\\ &+\frac{k\epsilon^2}{2}\left(\Delta_h w^{n+1}+\Delta_h w^n\right) = \phi^n - k\left(\frac{3}{2}\Delta_h\phi^n - \frac{1}{2}\Delta_h\phi^{n-1}\right),\end{aligned} \tag{5.15}$$

where w^{n+1} is periodic. Finally, the second-order finite difference version of (4.4) is as follows: given ϕ^{n-1}, ϕ^n, $w^n \in \mathcal{C}^+_{m_x\times m_y}$ periodic, find $\phi^{n+1} \in \mathcal{C}^+_{m_x\times m_y}$ periodic such that

$$\begin{aligned}\phi^{n+1} &- \frac{k}{4}\left[\mathfrak{d}_x\left\{r^{n+1}\mathfrak{D}_x\phi^{n+1}\right\} + \mathfrak{d}_y\left\{r^{n+1}\mathfrak{D}_y\phi^{n+1}\right\} + \mathfrak{d}_x\left\{r^n\mathfrak{D}_x\phi^n\right\} + \mathfrak{d}_y\left\{r^n\mathfrak{D}_y\phi^n\right\}\right]\\ &- \frac{k}{12}\left[\mathfrak{d}_x\left\{r^{n+1}\mathfrak{D}_x\phi^n\right\} + \mathfrak{d}_y\left\{r^{n+1}\mathfrak{D}_y\phi^n\right\} + \mathfrak{d}_x\left\{r^{n+1}\mathfrak{D}_x\phi^n\right\} + \mathfrak{d}_y\left\{r^{n+1}\mathfrak{D}_y\phi^n\right\}\right]\\ &- \frac{k}{6}\left[\mathfrak{d}_x\left\{\hat{r}^{n+1}\left(\mathfrak{D}_x\phi^{n+1}+\mathfrak{D}_x\phi^n\right)\right\} + \mathfrak{d}_y\left\{\hat{r}^{n+1}\left(\mathfrak{D}_y\phi^{n+1}+\mathfrak{D}_y\phi^n\right)\right\}\right]\\ &+ \frac{k\epsilon^2}{2}\left(\Delta_h w^{n+1}+\Delta_h w^n\right) = \phi^n - k\left(\frac{3}{2}\Delta_h\phi^n - \frac{1}{2}\Delta_h\phi^{n-1}\right),\end{aligned} \tag{5.16}$$

where $\hat{r}^{n+1} := \mathfrak{D}_x\phi^{n+1}\cdot\mathfrak{D}_x\phi^n + \mathfrak{D}_y\phi^{n+1}\cdot\mathfrak{D}_y\phi^n \in \mathcal{V}_{m_x\times m_y}$, and the other quantities are the same as defined above.

We now define some grid inner products and norms:

$$(\phi\|\psi) = \sum_{i=1}^{m}\sum_{j=1}^{n}\phi_{i,j}\psi_{i,j}, \quad \phi,\,\psi \in \mathcal{C}_{m_x\times m_y}\cup\mathcal{C}^+_{m_x\times m_y}, \tag{5.17}$$

$$\begin{aligned}\langle u\|v\rangle = \frac{1}{4}\sum_{i=1}^{m}\sum_{j=1}^{n}\big(&u_{i+1/2,j+1/2}v_{i+1/2,j+1/2} + u_{i-1/2,j+1/2}v_{i-1/2,j+1/2}\\ &+ u_{i+1/2,j-1/2}v_{i+1/2,j-1/2} + u_{i-1/2,j-1/2}v_{i-1/2,j-1/2}\big),\\ &u,\,v \in \mathcal{V}_{m_x\times m_y},\end{aligned} \tag{5.18}$$

$$[f\|g]_{\rm ew} = \frac{1}{2}\sum_{i=1}^{m}\sum_{j=1}^{n}\left(f_{i+1/2,j}g_{i+1/2,j} + f_{i-1/2,j}g_{i-1/2,j}\right), \quad f,\,g \in \mathcal{E}^{\rm ew}_{m_x\times m_y}, \tag{5.19}$$

$$[f\|g]_{\rm ns} = \frac{1}{2}\sum_{i=1}^{m}\sum_{j=1}^{n}\left(f_{i,j+1/2}g_{i,j+1/2} + f_{i,j-1/2}g_{i,j-1/2}\right), \quad f,\,g \in \mathcal{E}^{\rm ns}_{m_x\times m_y}. \tag{5.20}$$

If $\phi \in \mathcal{C}_{m_x\times m_y}\cup\mathcal{C}^+_{m_x\times m_y}$, then $\|\phi\|_2 := \sqrt{h^2\,(\phi\|\phi)}$, and for all $\phi \in \mathcal{C}^+_{m_x\times m_y}$, define

$$\|\nabla_h\phi\|_2 := \sqrt{h^2\,[D_x\phi\|D_x\phi]_{\rm ew} + h^2\,[D_y\phi\|D_y\phi]_{\rm ns}}. \tag{5.21}$$

We now can establish the following summation-by-parts formulae for periodic grid functions. We omit the proofs for the sake of brevity.

PROPOSITION 5.1. *Let $\phi \in \mathcal{C}^+_{m_x \times m_y}$ and $u \in \mathcal{V}_{m_x \times m_y}$ be periodic grid functions. Then*

$$h^2 \, \langle \mathfrak{D}_x \phi \| u \rangle = -h^2 \, (\phi \| \mathfrak{d}_x u) \quad \textit{and} \quad h^2 \, \langle \mathfrak{D}_y \phi \| u \rangle = -h^2 \, (\phi \| \mathfrak{d}_y u) \, . \tag{5.22}$$

If $\phi \in \mathcal{C}^+_{m_x \times m_y}$, $f \in \mathcal{E}^{\mathrm{ew}}_{m_x \times m_y}$, and $g \in \mathcal{E}^{\mathrm{ns}}_{m_x \times m_y}$ are periodic grid functions, then

$$h^2 \, [D_x \phi \| f]_{\mathrm{ew}} = -h^2 \, (\phi \| d_x f) \quad \textit{and} \quad h^2 \, [D_y \phi \| f]_{\mathrm{ns}} = -h^2 \, (\phi \| d_y f) \, . \tag{5.23}$$

Let ϕ, $\psi \in \mathcal{C}^+_{m_x \times m_y}$ be periodic. Then

$$h^2 \, [D_x \phi \| D_x \psi]_{\mathrm{ew}} + h^2 \, [D_y \phi \| D_y \psi]_{\mathrm{ns}} = -h^2 \, (\phi \| \Delta \psi) \quad \textit{and} \quad h^2 \, (\phi \| \Delta \psi) = h^2 \, (\Delta \phi \| \psi) \, . \tag{5.24}$$

Now, a discrete energy corresponding to (1.5) may be defined as

$$E_h(\phi) := \frac{h^2}{4} \left\langle \left(\left(\mathfrak{D}_x \phi \right)^2 + \left(\mathfrak{D}_y \phi \right)^2 \right)^2 + \mathbf{1} \middle\| \mathbf{1} \right\rangle - \frac{1}{2} \left\| \nabla_h \phi \right\|_2^2 + \frac{\epsilon^2}{2} \left\| \Delta_h \phi \right\|_2^2 \tag{5.25}$$

for all $\phi \in \mathcal{C}^+_{m_x \times m_y}$. Using the summation-by-parts formulae just given, and the techniques for the space continuous case, we can establish the following result.

COROLLARY 5.2. *The schemes* (5.15) *and* (5.16) *are second-order accurate in time and space and unconditionally stable. More precisely, we find*

$$\begin{aligned} E_h \left(\phi^{n+1} \right) + \frac{1}{4} \left\| \nabla_h (\phi^{n+1} - \phi^n) \right\|_2^2 + \frac{1}{k} \left\| \phi^{n+1} - \phi^n \right\|_2^2 + \frac{1}{4} \left\| \nabla_h \left(\phi^{n+1} + \phi^{n-1} - 2\phi^n \right) \right\|_2^2 \\ = E_h \left(\phi^n \right) + \frac{1}{4} \left\| \nabla_h \left(\phi^n - \phi^{n-1} \right) \right\|_2^2 . \end{aligned} \tag{5.26}$$

Both schemes are uniquely solvable. The scheme (5.16) *enjoys the additional property that it is the Euler–Lagrange equation for a strictly convex, coercive variation problem (in finite dimensions).*

Because of the last fact, solving the scheme (5.16) is equivalent to minimizing a coercive, strictly convex functional, $E_{h,scheme}(\phi)$—whose exact form we omit for brevity—at each time step. To compute the results given in section 6 we use the simple Polak–Ribiére variant of the nonlinear conjugate gradient method for the minimization step [23]. In our implementation, in contrast to what is usually done (see, e.g., [1, 2]), we avoid using Brent's method in the line search stage, since it uses only information about the function to be minimized, namely, $E_{h,scheme}(\phi)$. (Note also that since Brent's method is a comparison method, line minimizers are found with, at best, only single-precision precision accuracy.) In place of Brent's method for line search (that is, line minimization of $E_{h,scheme}(\phi)$) we directly use the gradient information and a secant method to do the line search. In other words, instead of finding a line minimizer, we perform the equivalent operation of finding a line zero of the gradient, and to do the latter we use a simple secant method. This can be expressed as

$$\bar{\alpha} = \mathrm{argmin}_\alpha E_{h,scheme}(\phi + \alpha\zeta) = \mathrm{argzero}_\alpha \left(\delta_\phi E_{h,scheme}(\phi + \alpha\zeta) \| \zeta \right) , \tag{5.27}$$

where ζ is a given search direction and $\alpha \in \mathbb{R}$. Setting

$$g(\alpha) := \left(\delta_\phi E_{h,scheme}(\phi + \alpha\zeta) \| \zeta \right) , \tag{5.28}$$

we employ the secant search scheme

$$\alpha_{\ell+1} = \alpha_\ell - \frac{g(\alpha_\ell)}{s_\ell}, \quad s_\ell = \frac{g(\alpha_\ell) - g(\alpha_{\ell-1})}{\alpha_\ell - \alpha_{\ell-1}}. \tag{5.29}$$

We have the guaranteed convergence $\lim_{\ell\to\infty} \alpha_\ell = \bar{\alpha}$ due to strict convexity. In this way, we need not ever actually assemble or compute the functional $E_{h,scheme}(\phi)$.

5.2. Spatial discretization via Galerkin methods. Although the numerical results we present later in section 6 are obtained using the finite difference method of the previous subsection, for completeness we now discuss some Galerkin strategies for spatial discretization. The present discussion shows the flexibility of the proposed schemes and further emphasizes the point that what is most important for the stability of the schemes is the structure of the temporal discretization.

To begin, notice that the proof of Theorem 2.1 (respectively, Theorem 3.1) is based on the weak forms (2.7) (respectively, (3.4)). Therefore, the results of Theorem 2.1 (respectively, Theorem 3.1) can be straightforwardly extended for any consistent Galerkin approximation—such as the Fourier–Galerkin and finite element Galerkin approximations—of the semidiscrete scheme (2.7) (respectively, (3.4)). The only modification needed is to view the "energy" as defined on the finite dimensional Galerkin space, compute the variational derivatives within the same Galerkin projected space, and view the fully discrete scheme as time discretization of a gradient flow on the finite dimensional Galerkin projected space.

From this point of view, Galerkin methods are in a sense more natural than the finite difference method, because the theory and analyses extend almost trivially. On the other hand, in contrast with finite difference methods, the implementation of such schemes is a more challenging task. We now consider the ingredients for a practical Fourier–Galerkin implementation.

5.3. Fourier–Galerkin method with numerical integration. While the results of Theorem 2.1 (respectively, Theorem 3.1) hold for Fourier–Galerkin approximation to (2.7) (respectively, (3.4)), it is usually not practical to implement a pure Fourier–Galerkin method due to the convolution involved in computing nonlinear terms. A common practice is to replace the integral by a numerical quadrature, leading to the so-called Fourier–Galerkin method with numerical integration.

We now sketch some details of the Fourier–Galerkin method with numerical integration. For simplicity, we shall consider only the alternative scheme for the case with slope selection, namely, the scheme (4.5). The Fourier–Galerkin method with numerical integration for other schemes can be formulated in a similar fashion. Let us first write the scheme (4.5) in the following weak form: find $\phi^{n+1} \in \dot{H}^2{}_{per}(\Omega)$ such that

$$\begin{aligned}\left(\frac{\phi^{n+1}-\phi^n}{k}, \psi\right) = &-\frac{1}{4}\left((|\nabla\phi^{n+1}|^2 + |\nabla\phi^n|^2)(\nabla\phi^{n+1} + \nabla\phi^n), \nabla\psi\right) \\ &+ \left(\nabla\left(\frac{3}{2}\phi^n - \frac{1}{2}\phi^{n-1}\right), \nabla\psi\right) - \frac{\epsilon^2}{2}(\Delta(\phi^{n+1} + \phi^n), \Delta\psi) \\ &\forall \psi \in \dot{H}^2{}_{per}(\Omega).\end{aligned} \tag{5.30}$$

Given an even integer N, we set

$$P_N = \left\{ \phi : \phi(x) = \sum_{k=1}^{N/2} (\tilde{a}_k \cos kx + \tilde{b}_k \sin kx) \right\} \tag{5.31}$$

and $x_j = \frac{2\pi j}{N}$, $j = 0, 1, \ldots, N-1$. We also define the discrete inner product P_N as

$$(\phi, \psi)_N = \frac{2\pi}{N} \sum_{j=0}^{N-1} \phi(x_j)\psi(x_j), \tag{5.32}$$

and the corresponding discrete norm by $\|\phi\|_N = \sqrt{(\phi, \phi)_N}$. We recall that the above quadrature rule is exact for $\phi, \psi \in P_{2N}$, i.e.,

$$(\phi, \psi)_N = (\phi, \psi) \quad \forall \phi, \psi \in P_{2N}, \tag{5.33}$$

and consequently,

$$\|\phi\|^2 = (\phi, \phi)_N \quad \forall \phi \in P_N. \tag{5.34}$$

In the multidimensional case, $\Omega = (0, \pi)^d$, $d = 2, 3$, we denote $x_{\mathbf{j}} = \Pi_{k=1}^d x_{j_k}$ with $0 \le j_k \le N-1$, $P_{\mathbf{N}} = \Pi_{k=1}^d P_N$, and

$$(\phi, \psi)_{\mathbf{N}} = \left(\frac{2\pi}{N}\right)^d \sum_{k=1}^{d} \sum_{j_k=0}^{N-1} \phi(x_{j_k})\psi(x_{j_k}). \tag{5.35}$$

With the above notation, we can now write our Fourier–Galerkin method with numerical integration for the scheme (5.30) as follows: find $\phi_N^{n+1} \in P_{\mathbf{N}}$ such that

$$\begin{aligned}\left(\frac{\phi_N^{n+1} - \phi_N^n}{k}, \psi\right) = &-\frac{1}{4}\left((|\nabla\phi_N^{n+1}|^2 + |\nabla\phi^n|^2)(\nabla\phi_N^{n+1} + \nabla\phi_N^n), \nabla\psi\right)_{\mathbf{N}} \\ &+ \left(\nabla\left(\frac{3}{2}\phi_N^n - \frac{1}{2}\phi_N^{n-1}\right), \nabla\psi\right) - \frac{\epsilon^2}{2}(\Delta(\phi_N^{n+1} + \phi_N^n), \Delta\psi) \\ &\qquad \forall \psi \in P_{\mathbf{N}}.\end{aligned} \tag{5.36}$$

Using the same argument as in the proof of Theorem 3.1, we can prove the following results.

COROLLARY 5.3. *The scheme* (5.36) *is second-order accurate in time, uniquely solvable, and unconditionally energy stable in the sense that*

$$\begin{aligned}E_N(\phi_N^{n+1}) + \frac{1}{4}\|\nabla(\phi_N^{n+1} - \phi_N^n)\|^2 + \frac{\|\phi_N^{n+1} - \phi_N^n\|^2}{k} + \frac{1}{4}\|\nabla(\phi_N^{n+1} + \phi_N^{n-1} - 2\phi_N^n)\|^2 \\ = E_N(\phi_N^n) + \frac{1}{4}\|\nabla(\phi_N^n - \phi_N^{n-1})\|^2,\end{aligned} \tag{5.37}$$

where

$$E_N(\phi) = \frac{1}{4}\|(|\nabla\phi|^2 - 1)\|_{\mathbf{N}}^2 + \frac{\epsilon^2}{2}\|\Delta\phi\|^2.$$

We observe that the weak formulation (5.36) can be intepreted as a Fourier-collocation method thanks to the exactness of the quadrature (5.33). To this end, we introduce the Lagrange functions $\psi_j(x) \in P_N$ such that $\psi_j(x_k) = \delta_{kj}$ for all $0 \le k, j \le N-1$, and denote by D_N the derivative matrix with $(D_N)_{jl} := \psi_l'(x_j)$. It is shown (see, for example, [3]) that

$$(D_N)_{jl} = \begin{cases} \frac{1}{2}(-1)^{j+l} \cot\frac{(j-l)\pi}{N}, & j \ne l, \\ 0, & j = l. \end{cases} \tag{5.38}$$

Therefore, for $\phi \in P_N$, we have $\phi'(x_j) = \sum_{k=0}^{N-1}(D_N)_{jk}\phi(x_k)$. In the multidimensional case, it is clear that for $\phi \in P_{\mathbf{N}}$, $(\nabla\phi)(x_{\mathbf{j}})$ can be expressed by using the one-dimensional derivative matrix D_N. We can then denote $(\nabla\phi)(x_{\mathbf{j}}) = (\nabla_{\mathbf{N}}\phi)_{\mathbf{j}}$, where $\nabla_{\mathbf{N}}$ is the multidimensional derivative matrix. Similarly, we denote $(\Delta\phi)(x_{\mathbf{j}}) = (\Delta_{\mathbf{N}}\phi)_{\mathbf{j}}$.

Now, it is easy to check that the scheme (5.36) is equivalent to the following Fourier-collocation method:

$$\begin{aligned}\frac{\phi_N^{n+1}-\phi_N^n}{k} &= \frac{1}{4}\nabla_{\mathbf{N}}\cdot\left((|\nabla_N\phi_N^{n+1}|^2+|\nabla_N\phi^n|^2)(\nabla_{\mathbf{N}}\phi_N^{n+1}+\nabla_{\mathbf{N}}\phi_N^n)\right)\\ &\quad-\nabla_{\mathbf{N}}\left(\frac{3}{2}\phi_N^n-\frac{1}{2}\phi_N^{n-1}\right)-\frac{\epsilon^2}{2}\Delta_{\mathbf{N}}^2(\phi_N^{n+1}+\phi_N^n),\end{aligned} \tag{5.39}$$

where, with a slight abuse of notation, ϕ_N^n are vectors with entries being the values of ϕ_N^n at the collocation points $\{x_{\mathbf{j}} : 0 \le j_k \le N-1, k = 1,\dots,d\}$.

6. Numerical results. In this section we present some computational results for the slope selection equation, i.e., (1.5)–(1.7) or (5.1). Specifically, we use our second-order finite difference scheme (5.16) described in section 5.1 with the simple nonlinear conjugate gradient solver described therein to solve the algebraic equations at each time step. We first present a numerical test that gives evidence of the expected second-order convergence of the scheme as h, $k \to 0$. In a second test, we reproduce some calculations from a previous paper [30] to show that in long-time calculations the scheme predicts the accepted coarsening rates for the system.

As in [14] we perform a Cauchy-type convergence test of our scheme as h, $k \to 0$ along a linear refinement path, namely, $k = Ch$. At the final time T, we expect the global error to be $O(k^2)+O(h^2) = O(h^2)$, as h, $k \to 0$, along such a path [18]. Observe that the evolution equation (5.1) does not possess a natural time-dependent forcing (or source) term that can be manipulated given a known solution (although one could be easily added artificially). So instead of measuring the error with respect to a known function via artificial means, we measure the Cauchy difference, $\delta_\phi(T) := \phi_{h_f}^{N_f} - \phi_{h_c}^{N_c}$, where $h_c = 2h_f$, $k_c = 2k_f$, $T = k_fN_f = k_cN_c$, as h_c, $k_c \to 0$. Here ϕ_{h_f} is the finite difference solution obtained using the finer resolution mesh size h_f, and ϕ_{h_c} is the finite difference solution obtained using the coarser resolution mesh size h_c. Using a linear refinement path, we again expect $\|\delta_\phi\|_2 = O(h_c^2)$. Further details of the test can be gleaned from [14]. Another option in this case—where there is no natural forcing term to manipulate—is to compute the "exact" solution using very small time and space step sizes h and k and use such a hyperfine solution to calculate "errors" for more modest values of h and k. The same results are expected as would be expected from such a test.

For the proposed convergence test, we use the final time $T = 0.32$, and the refinement path is taken to be $k = 0.1h$. The other parameters are $\epsilon = 0.1$ and $L_x = L_y = 3.2$. The following periodic initial data are employed:

$$\begin{aligned}\phi(x,y,0) &= 0.1\sin^2\left(\frac{2\pi x}{L_x}\right)\cdot\sin\left(\frac{4\pi(y-1.4)}{L_y}\right)\\ &\quad-0.1\cos\left(\frac{2\pi(x-2.0)}{L_x}\right)\cdot\sin\left(\frac{2\pi y}{L_y}\right).\end{aligned} \tag{6.1}$$

TABLE 6.1

L^2 Cauchy convergence test. The final time is $T = 0.32$, and the refinement path is taken to be $k = 0.1h$. The other parameters are $\epsilon = 0.1$; $L_x = L_y = 3.2$. The Cauchy difference is defined via $\delta_\phi := \phi_{h_f} - \phi_{h_c}$, where the approximations are evaluated at time $t = T$. The norm of the Cauchy difference at T is expected to be $\mathcal{O}(k^2) + \mathcal{O}(h^2) = \mathcal{O}(h^2)$, and this is confirmed in the test.

h_c	h_f	$\|\delta_\phi\|_{L_h^2}$	Rate
$1/16$	$1/32$	4.844×10^{-2}	–
$1/32$	$1/64$	1.373×10^{-2}	1.82
$1/64$	$1/128$	3.478×10^{-3}	1.98
$1/128$	$1/256$	8.675×10^{-4}	2.00

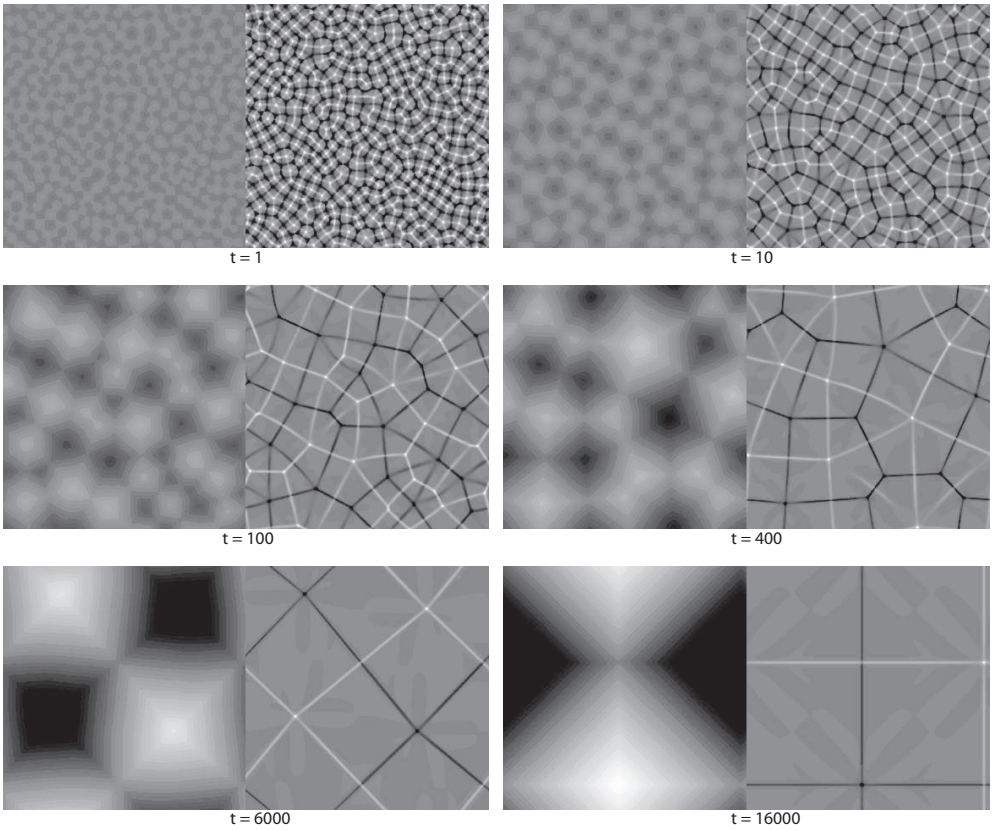

FIG. 6.1. *Time snapshots of the evolution of the model with slope selection. The parameters are $\epsilon = 0.03$; $L_x = L_y = 12.8$; $h = 12.8/512$; $k = 0.001$, $t \in [0, 400]$; $k = 0.01$, $t \in [4000, 6000]$; and $k = 0.02$, $t \in [6000, 16000]$. The left-hand sides of the snapshots show the filled contour plot of ϕ; the right-hand sides show the filled contour plot of $\Delta\phi$. The latter gives an indication of the curvature of the surface $z = \phi(x, y)$. The pyramid/antipyramid shapes of the hills and valleys are evident in the plots. The system clearly saturates (to a one-hill-one-valley configuration) by time* 16,000.

The results are given in Table 6.1 and give solid supporting evidence for the expected second-order convergence of the scheme.

We now reproduce a calculation from [30] where we use the scheme to predict the coarsening exponents for the slope selection equation (5.1) on a square domain beginning with random initial data. The results are given in Figures 6.1–6.3. The

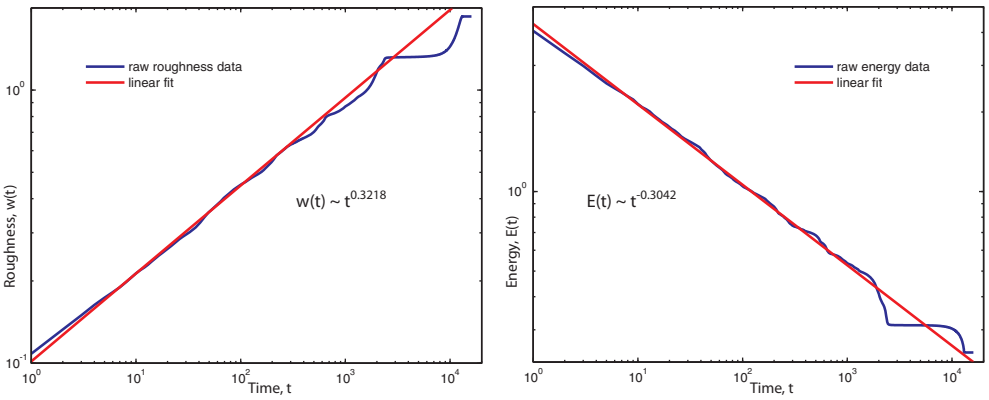

FIG. 6.2. *Roughness and energy evolution for the simulation depicted in Figure* 6.1. *The final simulation time is* $T = 16000$. *The theoretical coarsening exponents are* $\alpha = 1/3$ *and* $\beta = -1/3$, *where the roughness evolves like* $w(t) \sim t^{\alpha}$, *and the energy, like* $E(t) \sim t^{\beta}$. *These exponents are reasonably well approximated in the simulations.*

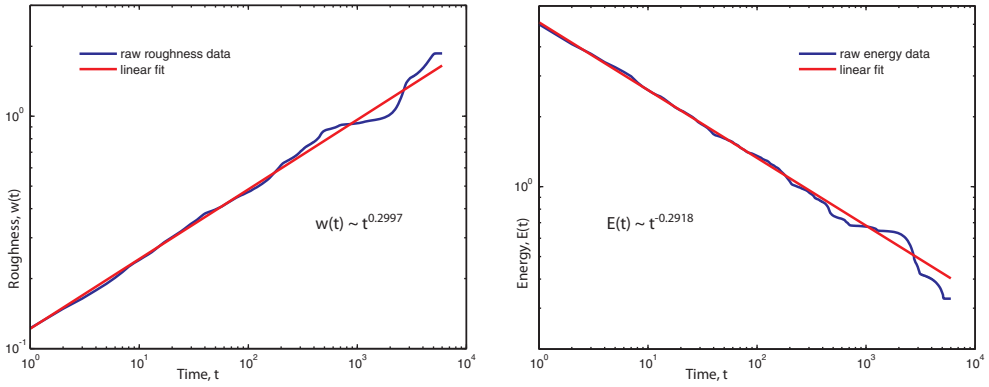

FIG. 6.3. *Roughness and energy evolution for* $\epsilon = 0.04$. *The final simulation time is* $T = 2300$. *All other parameters are the same as in Figures* 6.1 *and* 6.2. *The theoretical coarsening exponents* $\alpha = 1/3$ *and* $\beta = -1/3$ *are reasonably well approximated in the simulations.*

parameters are $\epsilon = 0.03$ (Figures 6.1 and 6.2) and $\epsilon = 0.04$ (Figure 6.3); $L_x = L_y = 12.8$; $h = 12.8/512$; $k = 0.001$, $t \in [0, 400]$; $k = 0.01$, $t \in [4000, 6000]$; and $k = 0.02$, $t \in [6000, 16000]$. Note that the computation in Figure 6.3 is finished by time $t = 6000$. The pyramid/antipyramid shapes of the hills and valleys are evident in Figure 6.1, and the slopes of the faces of the pyramids are approximately 1. The system depicted in Figure 6.1 clearly saturates (to a one-hill-one-valley configuration) by time 16,000. (A similar one-hill-one-valley configuration represents the equilibrium state for $\epsilon = 0.04$ as well, though this is not shown.) Roughly speaking, the saturation time can be gleaned from Figure 6.2 (or Figure 6.3 for the $\epsilon = 0.04$ case) as the time after which the roughness and energy are essentially flat. There are ways, as we discuss in [4], that one can use a linear extrapolation of the early-time data to obtain a cheap approximation of the saturation time. Basically, one uses the fact that $E_{\min}(\epsilon) = O(\epsilon)$, though we do not pursue this topic here. We do point out that our

calculations here yield

$$\frac{E_{\min}(\epsilon = 0.03)}{E_{\min}(\epsilon = 0.04)} \approx 0.7469, \tag{6.2}$$

which confirms the linear dependence of $E_{\min}$ on ϵ.

The theoretical coarsening exponents for the slope selection equation (as determined by formal scaling arguments) are $\alpha = 1/3$ and $\beta = -1/3$, where the roughness, i.e.,

$$w(t) = \sqrt{\frac{1}{|\Omega|}\int_{\Omega}\left|\phi(\mathbf{x},t) - \bar{\phi}(t)\right|^2 \mathrm{d}\mathbf{x}}, \tag{6.3}$$

evolves like $w(t) \sim O(t^{\alpha})$, and the energy (1.5) evolves like $E(t) \sim O(t^{\beta})$ [20]. (In fact, there is a sense in which these exponents may be established rigorously [17], though we do not need that level of detail here.) In Figures 6.2 and 6.3 we found the linear least-squares fit of the log-log data up to time $t = 100$. Using these fits, for $\epsilon = 0.03$ (Figure 6.2) we calculate $\alpha \approx 0.3218$ and $\beta \approx -0.3042$, and for $\epsilon = 0.04$ (Figure 6.3) we calculate $\alpha \approx 0.2997$ and $\beta \approx -0.2918$. Thus we observe that the coarsening exponents are reasonably well approximated in our simulations, and our figures agree with those found previously in [30]. This is also in accordance with earlier works [22, 27, 28, 32], although we have computed to a much longer time horizon (up to steady state), which leads to the "nonstraight" part of the coarsening curve.

7. Concluding remarks. We have presented and analyzed several second-order in time, uniquely solvable, unconditionally energy stable, and convergent schemes for gradient flows with Ehrlich–Schwoebel type energy. Applications to models for thin film epitaxial growth with or without slope selection are presented. There are two types of schemes: one type preserves the variational structure of the continuous in time gradient flow while the other does not. The ones without variational structure are usually more compact than the ones with variational structure. Fully discretized schemes with either Galerkin–Fourier-spectral or Fourier–Galerkin with numerical integration or finite difference in space are also presented and investigated. These fully discrete schemes inherit the same desirable properties as their semidiscrete in time counterparts, including second-order in time, unique solvability, and unconditional energy stability. We believe that the same methodology may be applied to more general energy functional.

Numerical experiments based on the scheme with variational structure and finite difference discretization of space are conducted on the model with slope selection. Our numerical results verifies the second-order accuracy as well as physical coarsening rates of the system.

It is still not clear if the scheme proposed here possesses a discrete energy law for general concave (not just quadratic) energy density. A positive answer would be useful since there exists splitting of the Ehrlich–Schwoebel energy with quadratic convex part and nonquadratic concave part for the case without slope selection. If, in general, the concave part can be treated explicitly, we will have a second-order linear scheme that is unconditionally energy stable for thin film epitaxy in the case without slope selection. This would be a nice extension of a result on first-order linear schemes that are unconditionally energy stable for the case without slope selection [4].

Acknowledgment. The financial support and warm hospitality of the Institute for Mathematics and Its Applications at the University of Minnesota are gratefully acknowledged.

REFERENCES

[1] J.W. Barrett and W.B. Liu, *Finite element approximation of the p-Laplacian*, Math. Comput., 61 (1993), pp. 523–537.

[2] J.W. Barrett and W.B. Liu, *Finite element approximation of the parabolic p-Laplacian*, SIAM J. Numer. Anal., 31 (1994), pp. 413–428.

[3] C. Canuto, Y.M. Hussaini, A. Quarteroni, and T.A. Zang, *Spectral Methods: Fundamentals in Single Domains*, Springer-Verlag, Berlin, 2006.

[4] W.B. Chen, S. Conde, C. Wang, X. Wang, and S. Wise, *A linear energy stable numerical scheme for epitaxial thin film growth model without slope selection*, J. Sci. Comput., in press.

[5] M. Cheng and J.A. Warren, *An efficient algorithm for solving the phase field crystal model*, J. Comput. Phys., 227 (2008), p. 6241.

[6] Q. Du and R. Nicolaides, *Numerical analysis of a continuum model of a phase transition*, SIAM J. Numer. Anal., 28 (1991), pp. 1310–1322.

[7] I. Ekeland and R. Témam, *Convex Analysis and Variational Problems*, SIAM, Philadelphia, 1999.

[8] G. Ehrlich and F.G. Hudda, *Atomic view of surface diffusion: Tungsten on tungsten*, J. Chem. Phys., 44 (1966), p. 1036.

[9] J.W. Evans and P.A. Thiel, *A little chemistry helps the big get bigger*, Science, 29 (2010), pp. 599–600.

[10] J.W. Evans, P.A. Thiel, and M.C. Bartelt, *Morphological evolution during epitaxial thin film growth: Formation of* $2D$ *islands and* $3D$ *mounds*, Surface Science Reports, 61 (2006), pp. 1–128.

[11] L.C. Evans, *Partial Differential Equations*, American Mathematical Society, Providence, RI, 1998.

[12] D.J. Eyre, *Computational and Mathematical Models of Microstructural Evolution*, J.W. Bullard et al., eds., MRS, Warrendale, PA, 1998, pp. 39–46.

[13] M. Giaquinta, *Multiple Integrals in the Calculus of Variations and Nonlinear Elliptic Systems*, Princeton University Press, Princeton, NJ, 1983.

[14] Z. Hu, S.M. Wise, C. Wang, and J.S. Lowengrub, *Stable and efficient finite-difference nonlinear-multigrid schemes for the phase field crystal equation*, J. Comput. Phys., 228 (2009), pp. 5323–5339.

[15] R.V. Kohn, *Energy-driven pattern formation*, in Proceedings of the International Congress of Mathematicians, Madrid, 2006.

[16] R.V. Kohn and F. Otto, *Upper bounds on coarsening rates*, Comm. Math. Phys., 229 (2002), pp. 375–395.

[17] R.V. Kohn and X. Yan, *Upper bound on the coarsening rate for an epitaxial growth model*, Comm. Pure Appl. Math., 56 (2003), pp. 1549–1564.

[18] R.J. LeVeque, *Finite Difference Methods for Ordinary and Partial Differential Equations, Steady State and Time Dependent Problems*, SIAM, Philadelphia, 2007.

[19] B. Li, *High-order surface relaxation versus the Ehrlich-Schwoebel effect*, Nonlinearity, 19 (2006), pp. 2581–2603.

[20] B. Li and J.-G. Liu, *Thin film epitaxy with or without slope selection*, European J. Appl. Math., 14 (2003), pp. 713–743.

[21] B. Li and J.-G. Liu, *Epitaxial growth without slope selection: Energetics, coarsening, and dynamic scaling*, J. Nonlinear Sci., 14 (2004), pp. 429–451.

[22] D. Moldovan and L. Golubovic, *Interfacial coarsening dynamics in epitaxial growth with slope selection*, Phys. Rev. E, 61 (2000), pp. 6190–6214.

[23] E. Polak and G. Ribiére, *Note sur la convergence des méthodes de directions conjuguées*, Rev. Fr. Imform. Res. Oper., 16 (1969), pp. 35–43.

[24] R.L. Schwoebel, *Step motion on crystal surfaces:* II, J. Appl. Phys., 40 (1969), p. 614.

[25] J. Shen and X. Yang, *Numerical approximations of Allen-Cahn and Cahn-Hilliard equations*, Discrete Contin. Dyn. Syst. Ser. A, 28 (2010), pp. 1669–1691.

[26] J. Shen and X. Yang, *A phase-field model and its numerical approximation for two-phase incompressible flows with different densities and viscosities*, SIAM J. Sci. Comput., 32 (2010), pp. 1159–1179.

[27] M. Siegert, *Ordering dynamics of surfaces in molecular beam epitaxy*, Phys. A, 239 (1997), pp. 420–427.

[28] M. Siegert and M. Plischke, *Slope selection and coarsening in molecular beam epitaxy*, Phys. Rev. Lett., 73 (1994), pp. 1517–1520.

[29] B.P. Vollmayr-Lee and A.D. Rutenberg, *Fast and accurate coarsening simulation with an unconditionally stable time step*, Phys. Rev. E, 68 (2003), p. 066703.

[30] C. Wang, S. Wang, and S.M. Wise, *Unconditionally stable schemes for equations of thin film epitaxy*, Disc. Contin. Dyn. Sys. Ser. A, 28 (2010), pp. 405–423.
[31] S.M. Wise, C. Wang, and J.S. Lowengrub, *An energy stable and convergent finite-difference scheme for the Phase Field Crystal equation*, SIAM J. Numer. Anal., 47 (2009), pp. 2269–2288.
[32] C. Xu and T. Tang, *Stability analysis of large time-stepping methods for epitaxial growth models*, SIAM J. Numer. Anal., 44 (2006), pp. 1759–1779.
[33] X. Ye, *The Legendre collocation method for the Cahn-Hilliard equation*, J. Comput. Appl. Math., 150 (2003), pp. 87–108.